LA-UR-17-24941

High-energy-density shear flow and instability experiments

F. W. Doss, K. A. Flippo, E. C. Merritt,
C. A. Di Stefano, B. G. DeVolder, S. Kurien,
J. L. Kline

SSGF meeting
June 22, 2017

Outline

- Motivation for studying shear-induced turbulence modeling in ICF-relevant regimes
- Demystification of turbulence modeling
- Sketch of the experiment
  - Design of the experiment
  - Evolution to NIF platform
  - Data we are getting out of it
- Preliminary results and conclusions

Classical mixing layers show the instability of shear flows (Kelvin-Helmholtz) evolving into 3D turbulence

2 *R. Breidenthal*

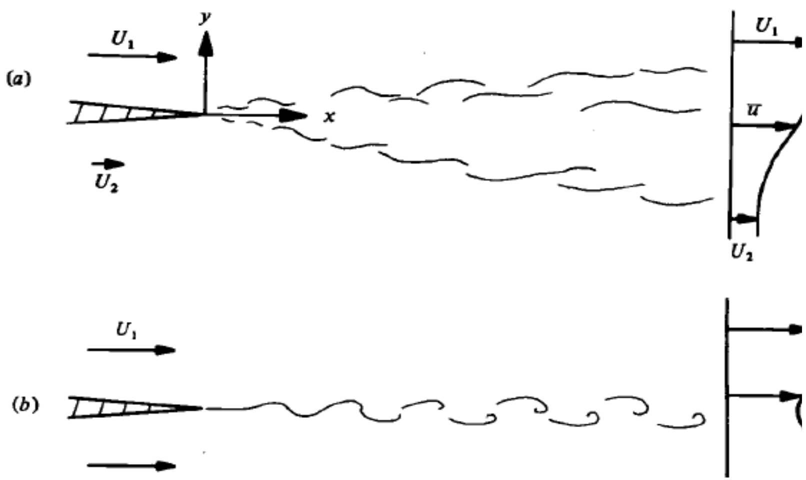

FIGURE 1. (a) Plane mixing layer. (b) Plane wake, thin trailing edge.

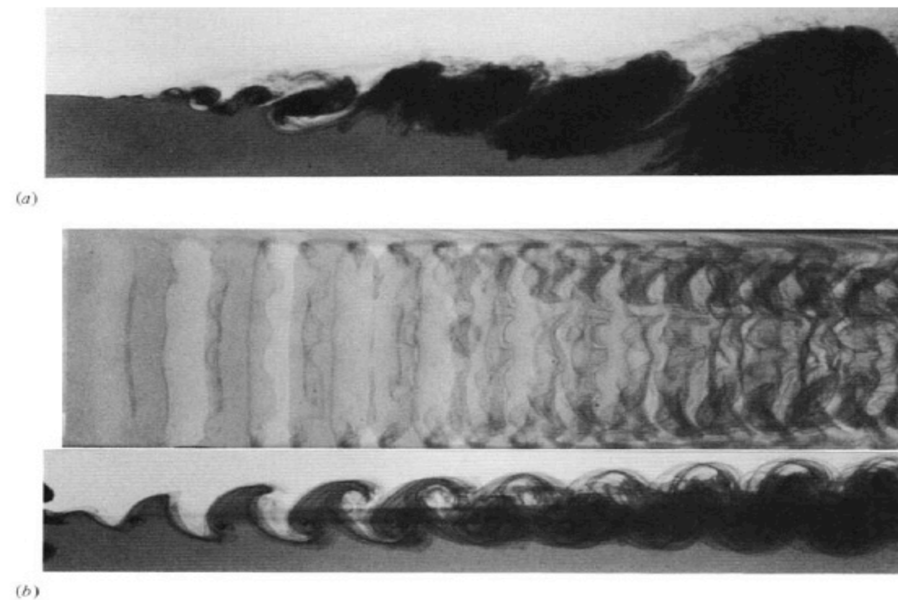

R. Breidenthal, "Structure in turbulent mixing layers and wakes using a chemical reaction," Journal of Fluid Mechanics **109**, 1 (1981).

In imploding capsules and astrophysical systems, classical hydrodynamics will eventually break down

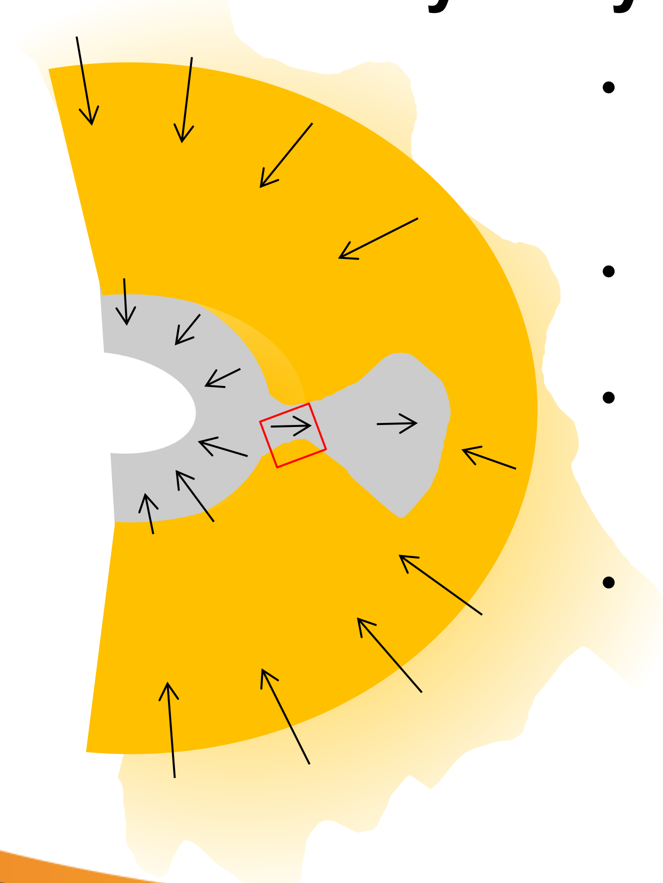

- For ICF implosions, the dominant instability is usually Rayleigh-Taylor, but shear is still present and playing a role.
- To include RT, turbulence models were extended beyond their classical applicability (BHR, others).
- Models are used to infer effects in the integrated systems, which are calibrated/informed by our experience in low-energy-density world.
- Other HED/ICF experiments have focused on linear instabilities (i.e. specific modes) in both Rayleigh-Taylor (or it's cousin Richtmyer-Meshkov) and Kelvin-Helmholtz geometries, but developed HED shear flow conditions were rare.

Experiments

Physics	Example
Low Atwood, low Mach number, weak shocks	Shock Tubes, Water Channels, etc.
Imploding hydrodynamics	High-Growth Radiography (Raman 2014) Wark, Kilkenny, et al Ap Phys Lett 1986
Laser-driven planar Rayleigh – Taylor	Cole, Kilkenny, et al Nature **299** 329 1982 Remington et al on NOVA, Phys Plas **4**
- Radiation–coupled	RadSNRT
RM – Reshock	Shock Tube reshock experiments LANL OMEGA Colliding Shock LLNL NIF ReShock
Laser-driven Shear	Hammel et al. Phys Plasmas **1**
Blast-wave driven KH	Hurricane-Harding OMEGA, Michigan OMEGA-EP
Laser-drive temporal mixing layer	LANL Shock/Shear (this talk) ⟵

Second order turbulence modeling in a nutshell

- Reynolds decomposition extracts a mean and a fluctuating quantity.
- Starting with the unperturbed Euler (Navier-Stokes without viscosity) equations:

$$\frac{\partial u_i}{\partial t} + u_j \cdot \frac{\partial u_i}{\partial x_j} = -\rho^{-1} \frac{\partial P}{\partial x_i}$$

- We make the replacement: $u_i \rightarrow U_i + u'_i$
- This gets us to the decomposed equations:

$$\frac{\partial U_i}{\partial t} + \frac{\partial u'_i}{\partial t} + U_j \frac{\partial U_i}{\partial x_j} + u'_j \frac{\partial U_i}{\partial x_j} + U_j \frac{\partial u'_i}{\partial x_j} + u'_j \frac{\partial u'_i}{\partial x_j} = -\rho^{-1} \frac{\partial P}{\partial x_i}$$

A comparison with linear perturbation theory - i

- So far, this is mathematically identical to linear perturbation extracting a mean and a perturbed quantity.
- The primed quantity is considered `small' and primed-squared quantities are dropped.

$$\frac{\partial U_i}{\partial t} + \frac{\partial u_i'}{\partial t} + U_j \frac{\partial U_i}{\partial x_j} + u_j' \frac{\partial U_i}{\partial x_j} + U_j \frac{\partial u_i'}{\partial x_j} + \cancel{u_j' \frac{\partial u_i'}{\partial x_j}} = -\rho^{-1} \frac{\partial P}{\partial x_i}$$

A comparison with linear perturbation theory - ii

- The linear perturbation analysis gives all information on wavelengths, phases, shapes of modes given a background.
- Linear Rayleigh-Taylor, Kelvin-Helmholtz, etc.
- But, it gives no information on feedback to the bulk flow (since the energy content has been set to infinitesimal for linearity to hold)

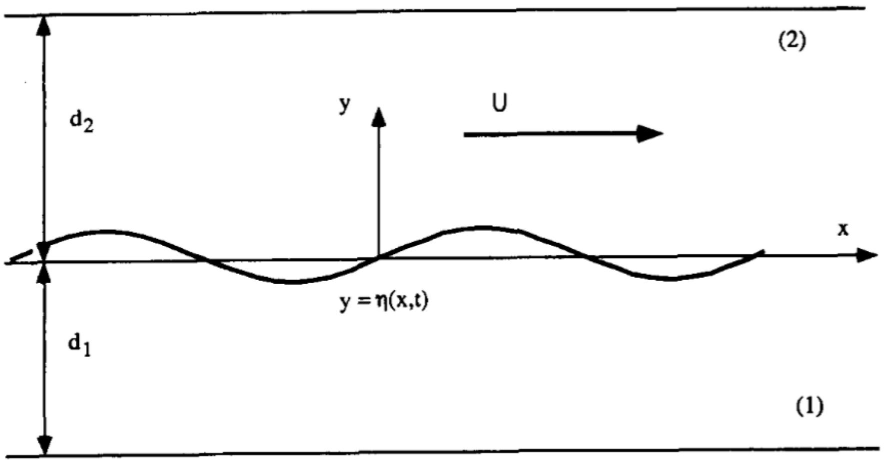

Int. J. Multiphase Flow Vol. 17, No. 4, pp. 509–518, 1991

Turbulence modeling occurs at the second-order level

- Instead, consider the primed term a fluctuation on top of a mean. Then perform an averaging operation and discard *single* powers of the primed variable.

$$\frac{\partial U_i}{\partial t} + \cancel{\frac{\partial u'_i}{\partial t}} + U_j \frac{\partial U_i}{\partial x_j} + \cancel{u'_j \frac{\partial U_i}{\partial x_j}} + \cancel{U_j \frac{\partial u'_i}{\partial x_j}} + u'_j \frac{\partial u'_i}{\partial x_j} = -\rho^{-1} \frac{\partial P}{\partial x_i}$$

- We have lost information about phase but retained information about average energy.

Rearranging gets the Reynolds equations

- If the flow is incompressible, then we write the feedback of the instability on the bulk flow as a divergence of the Reynolds stress tensor:

$$\frac{\partial U_i}{\partial t} + U_j \frac{\partial U_i}{\partial x_j} = -\frac{1}{\rho}\frac{\partial P}{\partial x_i} - \underbrace{\frac{\partial \langle u'_j u'_i \rangle}{\partial x_j}}_{\text{Reynolds stress}}$$

- This looks just like the old Euler equations, but with the new divergence of a tensor.
- This is called the Reynolds stress tensor, also denoted R_{ij}.

Original closures made the Reynolds stress look like a viscosity

- The eddy viscosity closure: (Boussinesq, 1877)

$$\langle u_x' u_y' \rangle \propto -\nu_T \left(\frac{\partial U_x}{\partial y} + \frac{\partial U_y}{\partial x} \right)$$

- This makes it look like the action of a viscosity since now

$$-\nabla \cdot \langle u_i' u_j' \rangle \propto \nu_T \nabla^2 U$$

- This is a reasonable approximation in 1D pipe flows, but less applicable in more complicated systems
- Modern approaches derive equations for either the full Reynolds stress tensor or its trace (*k*).

We get second-order equations for energy by moments of perturbed Euler

- We want an equation for $\dfrac{D\langle u'_i u'_j\rangle}{Dt} = \left\langle u'_i \dfrac{Du'_j}{Dt}\right\rangle + \left\langle u'_j \dfrac{Du'_i}{Dt}\right\rangle$
- Going back to the Reynolds-decomposed Euler equations,

$$\frac{\partial U_i}{\partial t} + \frac{\partial u'_i}{\partial t} + U_j\frac{\partial U_i}{\partial x_j} + u'_j\frac{\partial U_i}{\partial x_j} + U_j\frac{\partial u'_i}{\partial x_j} + u'_j\frac{\partial u'_i}{\partial x_j} = -\rho^{-1}\frac{\partial P}{\partial x_i}$$

we get the equations we are looking for by multiplying and averaging

$$\cancel{u'_j\frac{\partial U_i}{\partial t}} + u'_j\frac{\partial u'_i}{\partial t} + \cancel{u'_j U_k\frac{\partial U_i}{\partial x_k}} + u'_j u'_k\frac{\partial U_i}{\partial x_k} + \cancel{u'_j U_k\frac{\partial u'_i}{\partial x_k}} + u'_j u'_k\frac{\partial u'_i}{\partial x_k} = \cancel{-u'_j\rho^{-1}\frac{\partial P}{\partial x_i}}$$

Ignore *P* for now

We get second-order equations for energy by moments of perturbed Euler (ii)

$$\cancel{u'_j \frac{\partial U_i}{\partial t}} + u'_j \frac{\partial u'_i}{\partial t} + \cancel{u'_j U_k \frac{\partial U_i}{\partial x_k}} + u'_j u'_k \frac{\partial U_i}{\partial x_k} + \cancel{u'_j U_k} \frac{\partial u'_i}{\partial x_k} + u'_j u'_k \frac{\partial u'_i}{\partial x_k} = \cancel{-u'_j \rho^{-1}} \frac{\partial P}{\partial x_i}$$

- Adding the second copy of this equation with *i* <-> *j* gives:

$$\underbrace{\frac{\partial \langle u'_i u'_j \rangle}{\partial t} + U_k \frac{\partial \langle u'_i u'_j \rangle}{\partial x_k}}_{D_t \langle u'_i u'_j \rangle} = \underbrace{-\langle u'_i u'_k \rangle \frac{\partial U_j}{\partial x_k} - \langle u'_k u'_j \rangle \frac{\partial U_i}{\partial x_k}}_{\text{Production by shear}} - \frac{\partial \langle u'_i u'_j u'_k \rangle}{\partial x_k}$$

- Finally, the trace of this equation (*i* = *j*) gives the equation for *k*.

$$\frac{Dk}{Dt} = -\underbrace{\langle u'_i u'_j \rangle}_{\text{Close, or not}} \left(\frac{\partial U_i}{\partial x_j} + \frac{\partial U_j}{\partial x_i} \right) + \frac{\nu_T}{\sigma_k} \nabla^2 k$$

UNCLASSIFIED

We get second-order equations for energy by moments of perturbed N-S (iii)

$$\frac{Dk}{Dt} = -\langle u'_i u'_j \rangle \left(\frac{\partial U_i}{\partial x_j} + \frac{\partial U_j}{\partial x_i} \right) - \frac{\partial \langle u'_i u'_i u'_k \rangle}{\partial x_k}$$

- Closures are assigned as required,

$$\langle u'_i u'_i u'_k \rangle \propto -\nu_T \nabla k$$

$$\frac{Dk}{Dt} = -\underbrace{\langle u'_i u'_j \rangle}_{} \left(\frac{\partial U_i}{\partial x_j} + \frac{\partial U_j}{\partial x_i} \right) + \frac{\nu_T}{\sigma_k} \nabla^2 k$$

$$\langle u'_x u'_y \rangle \propto -\nu_T \left(\frac{\partial U_x}{\partial y} + \frac{\partial U_y}{\partial x} \right)$$

- And by dimensional analysis say that $\nu_T \propto l \cdot k^{1/2}$ where *l* is a length. If you just **specify** what *l* is everywhere, you get Prandtl's mixing length theory (1925).

UNCLASSIFIED

Various species of turbulence models for various degrees of sophistication

- If instead you write a dynamic equation for the scale *l* (not shown) you get two-equation models (Harlow & Nakayama, 'Turbulence Transport Equations,' *PoF* (1967))
- If you don't ignore the pressure term like we did earlier [Rotta 'Statistische Theorie nichthomogener Turbulenz,' *Z. Phys* (1953)] and solve for the entire tensor instead of reducing it to *k*, you can eliminate that eddy-viscosity approximation in the shear production [LRR, 'Development of a Reynolds-stress turbulence closure,' *JFM* (1975])
- If you **also** perturb density (ρ) by ρ' and derive equations for not only <u'u'> but also <u' ρ'> and some form of <ρ'ρ'>, you get BHR [Besnard, Harlow, Rauenzahn, "Conservation and transport properties of turbulence with large density variations" LA-10911-MS]

The BHR-2 four-equation turbulence model (BHR-3, in current use, has full tensor equations, but is longer)

Kinetic energy:
$$\frac{D\rho k}{Dt} = a_i \frac{\partial P}{\partial x_i} - R_{ij}\frac{\partial u_i}{\partial x_j} - \rho \frac{k^{3/2}}{s} + \text{diffusion}$$

Scale:
$$\frac{D\rho s}{Dt} = \frac{s}{k}\left[\left(\frac{3}{2} - c_4\right) a_i \frac{\partial P}{\partial x_i} - \left(\frac{3}{2} - c_1\right) R_{ij}\frac{\partial u_i}{\partial x_j}\right]$$
$$-c_3 \rho s \frac{\partial u_i}{\partial x_i} - \left(\frac{3}{2} - c_2\right)\rho k^{1/2} + \text{diffusion}$$

Mass flux:
$$\frac{D\rho a_i}{Dt} = b\frac{\partial P}{\partial x_i} - \frac{R_{ij}}{\rho}\frac{\partial \rho}{\partial x_j} - c_a \rho a_i \frac{k^{1/2}}{s} + \text{diffusion}$$

“b”:
$$\frac{D\rho b}{Dt} = 2\rho a_i \frac{\partial b}{\partial x_i} - 2(b+1)a_i\frac{\partial \rho}{\partial x_i} - c_b \rho b \frac{k^{1/2}}{s} + \text{diffusion}$$

Active scalars / **Treatment of flow**	**Flow only** (evolves $\langle u_i' u_j' \rangle$)	**Algebraic closure for density effects**	**Evolution equation for $\langle u_i' \rho' \rangle$ (*k*-L-a)**	**Evolution equation for $\langle \rho' \rho' \rangle / \langle \rho' \rho^{-1\prime} \rangle$ (*k*-L-a-*b*)**
One evolution equation (*k*)	Prandtl, 'Berict über Untersuchungen zur ausgbebildeten Turbulenz,' *Z. Angew. Math. Mech* (1925)	Andronov et al., 'Turbulent mixing at a contact surface accelerated by a shock wave,' *Zh. Eksp. Teor. Fiz.* (1976)		
Energy + scale (Two-equation *k*-ε/L/s/ω)	Harlow & Nakayama, 'Turbulence Transport Equations,' *PoF* (1967) Jones & Launder, 'Prediction of laminarization with a two-equation model of turbulence' *Int. J. H. M. Trans.* (1972)	Gauthier & Bonnet, 'A k–ε model for turbulent mixing in shock tube flows induced by RT,' *PoF* (1990) Dimonte & Tipton 'K-L model for self-similar growth of RT & RM' *PoF* (2006)	Morgan & Wickett 'Three-equation model for the self-similar growth of RT and RM instabilities' *PRE* (2015) Banerjee, Gore, Andrews, *PRE* (2010)	Ruffin et al., 'Characteristic scales in variable-density jets using a second-order model' *PoF* (1993)
Anisotropic effects, Reynolds stress tensor (R_{ij}–ε) Transient effects, two-scales (R_{ij}–ε_1–ε_2)	Rotta, 'Statistische Theorie nichthomogener Turbulenz,' *Z. Phys*. (1951) LRR, 'Development of a Reynolds-stress turbulence closure,' *JFM* (1975)			Schwarzkopf et al. *JoT* (2011), *Flow Turb. Comb* (2016) Grégoire, Souffland, Gauthier, 'A second-order turbulence model for gaseous mixtures' *JoT* (2005)

Active scalars / Treatment of flow	Flow only (evolves $\langle u_i' u_j' \rangle$)	Algebraic closure for density effects	Evolution equation for $\langle u_i' \rho' \rangle$ (*k*-L-a)	Evolution equation for $\langle \rho' \rho' \rangle / \langle \rho' \rho^{-1\prime} \rangle$ (*k*-L-a-*b*)
One evolution equation (*k*)	Prandtl, 'Berict über Untersuchungen zur ausgbebildeten Turbulenz,' *Z. Angew. Math. Mech* (1925)	Andronov et al., 'Turbulent mixing at a contact surface accelerated by a shock wave,' *Zh. Eksp. Teor. Fiz.* (1976)		
Energy + scale (Two-equation k-ε/L/s/ω)	Harlow & Nakayama, 'Turbulence Transport Equations,' *PoF* (1967) Jones & Launder, 'Prediction of laminarization with a two-equation model of turbulence' *Int. J. H. M. Trans.* (1972)	Gauthier & Bonnet, 'A k–ε model for turbulent mixing in shock tube flows induced by RT,' *PoF* (1990) Dimonte & Tipton 'K-L model for self-similar growth of RT & RM' *PoF* (2006)	Morgan & Wickett 'Three-equation model for the self-similar growth of RT and RM instabilities' *PRE* (2015) Banerjee, Gore, Andrews, *PRE* (2010)	Ruffin et al., 'Characteristic scales in variable-density jets using a second-order model' *PoF* (1993)
Anisotropic effects, Reynolds stress tensor (R_{ij}–ε) Transient effects, two-scales (R_{ij}–ε_1–ε_2)	Rotta, 'Statistische Theorie nichthomogener Turbulenz,' *Z. Phys.* (1951) LRR, 'Development of a Reynolds-stress turbulence closure,' *JFM* (1975)			Schwarzkopf et al. *JoT* (2011), *Flow Turb. Comb* (2016) Grégoire, Souffland, Gauthier, 'A second-order turbulence model for gaseous mixtures' *JoT* (2005)

"BHR-1"

"BHR-2"

"BHR-3"

Besnard, Harlow, Rauenzahn "Conservation and transport properties of turbulence with large density variations" LA-10911-MS

BHR (theory) 1987

We have fielded an experiment to study these models in a high-energy-density environment at OMEGA and NIF

Counterpropagating shear geometry

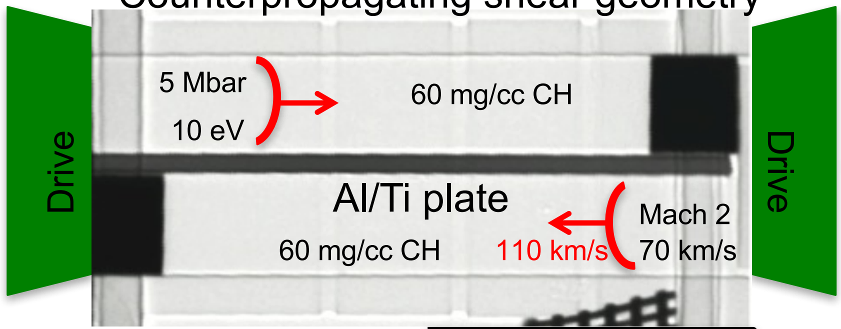

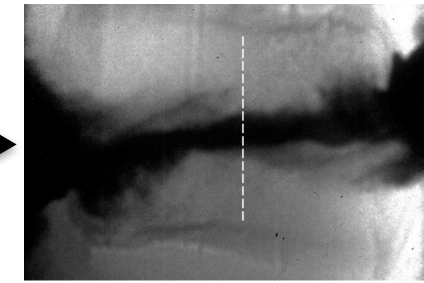

Mix width measured along line

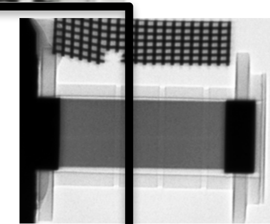

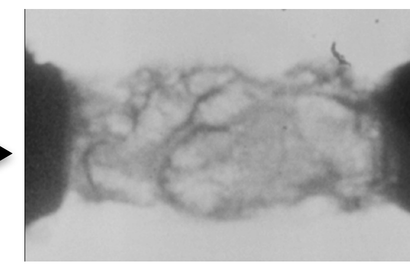

Orthogonal view

- To study shear in isolation, it is best to eliminate growth due to normal components.
- Counter-oriented shocks are used to symmetrize the experiment, establishing equal pressures above and below the tracer layer and eliminating drift effects.
- Top right: edge-on view measures tracer mix width, will be compared
  with RANS turbulence model predictions.
- Bottom right: orthogonal view is used to image the developing instability in the tracer plane.

Phys Plasmas, **20**, 012707 (2013)
Phys Plasmas, **20**, 122704 (2013)

Main observable is layer width as a function of time

Data published in *Phys Plasmas*, **20**, 122704 (2013)

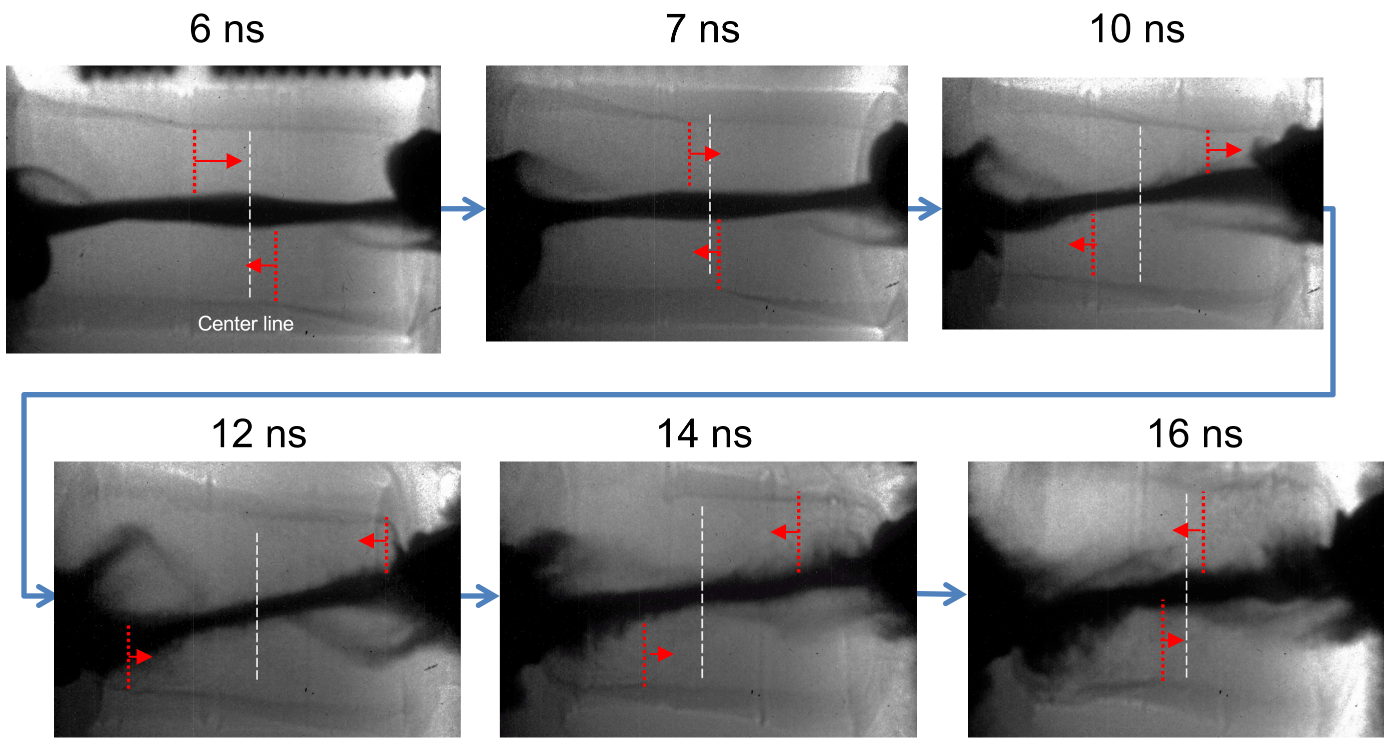

We are comparing this data to simulations in the LANL hydrocode RAGE

Simulations published in *Phys. Plasmas* **20**, 012707 (2013)

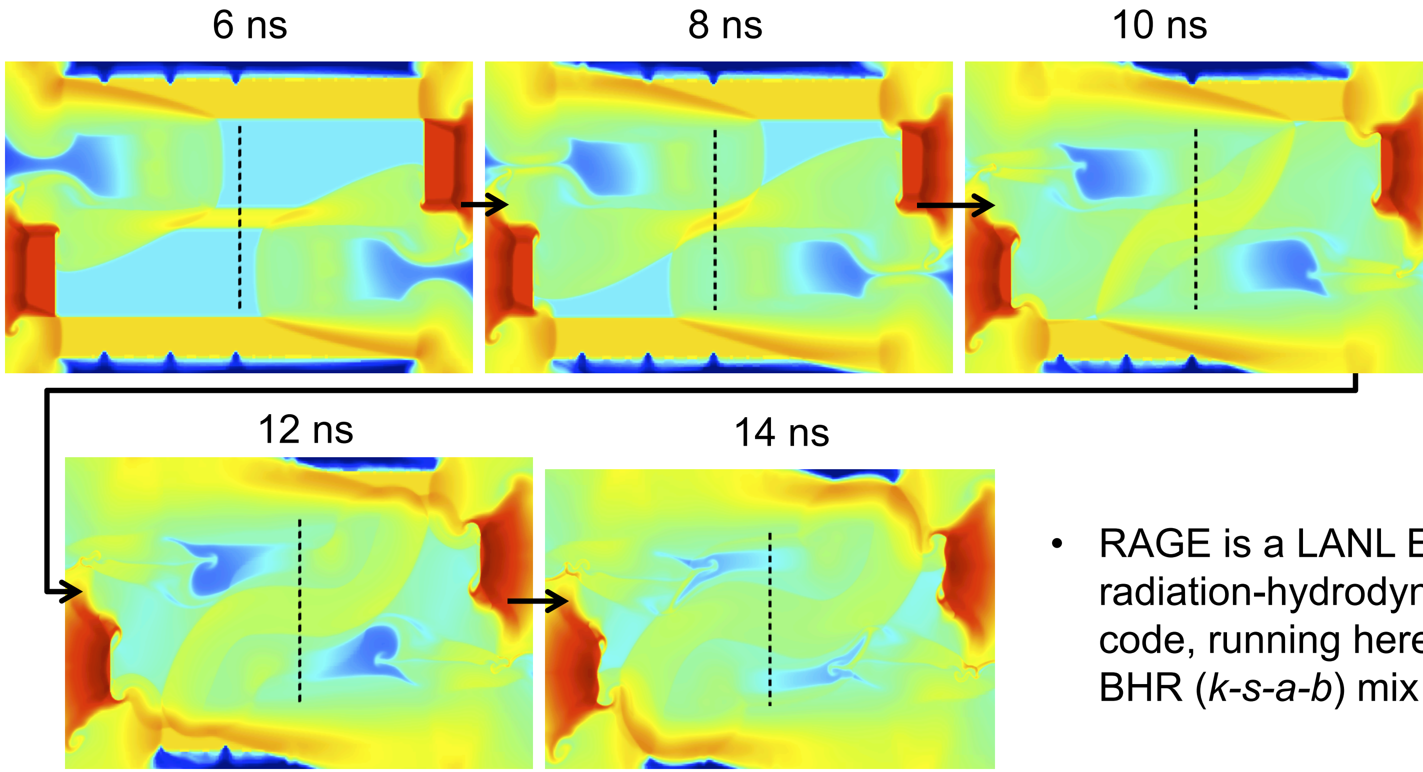

- RAGE is a LANL Eulerian radiation-hydrodynamics code, running here with the BHR (*k*-*s*-*a*-*b*) mix model.

Layer width over time is compared between simulation and experiment via synthetic radiography lineouts

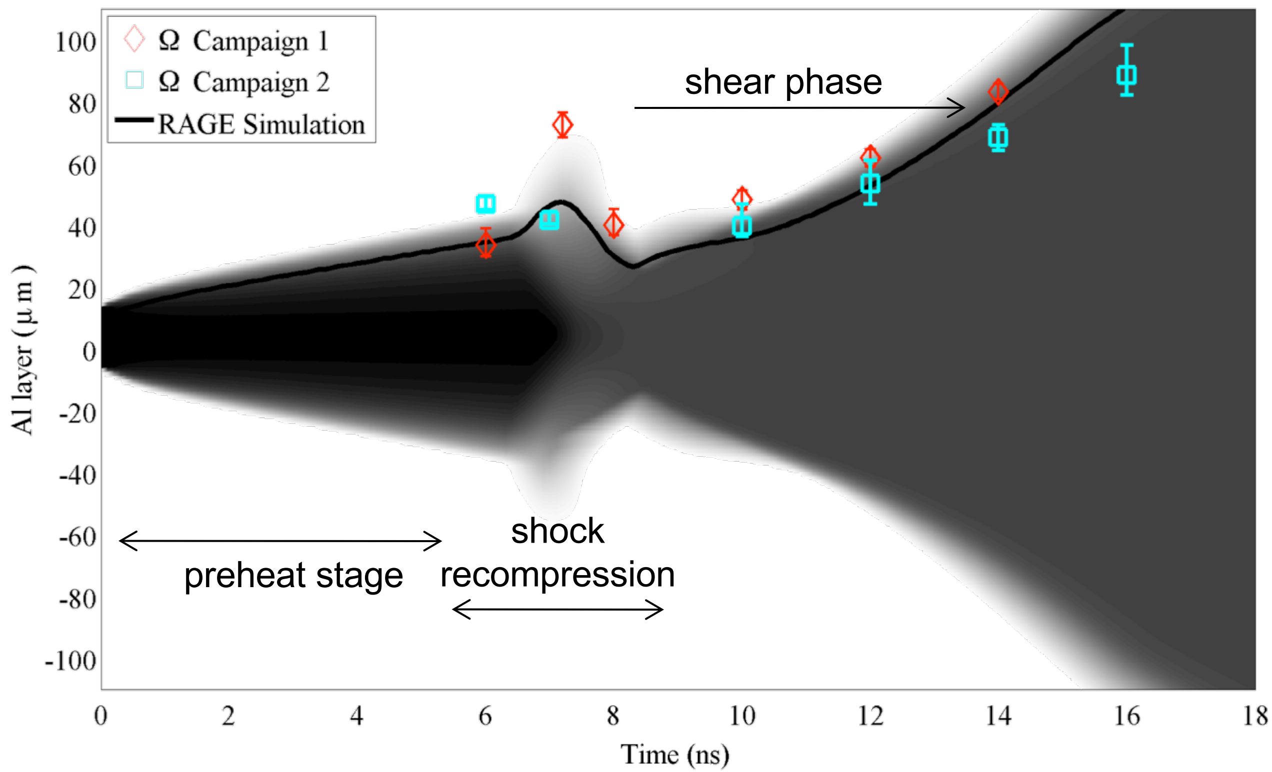

A clean (no mix) simulation does not show layer growth during the experiment lifetime

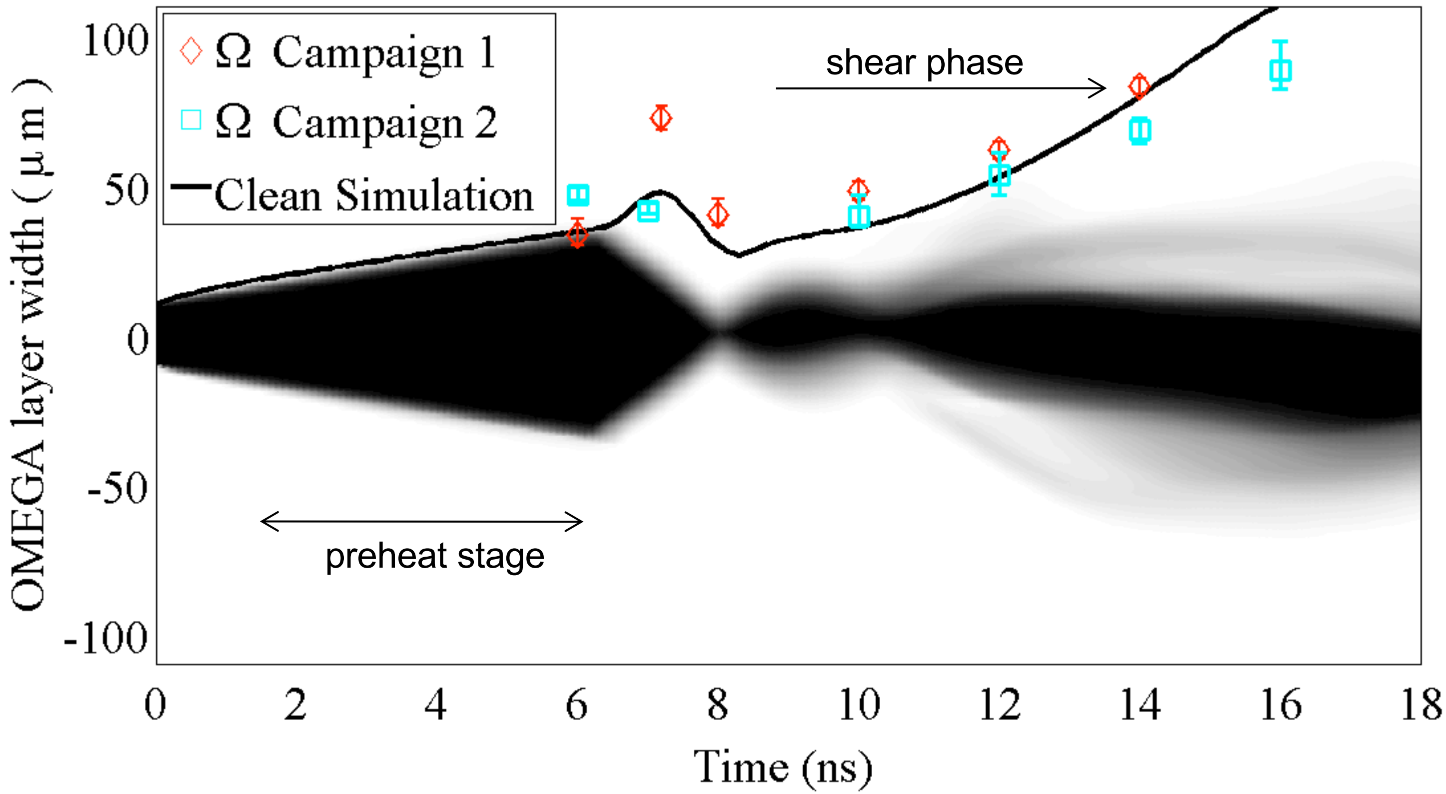

To eliminate transients and uncontrollable 3D features, we move to a larger, more steady experiment on NIF

- With >1 MJ available at NIF, compared to ~10 kJ at OMEGA, a much larger target can be constructed.
- Initial designs are scaled for same instability growth dynamics as OMEGA to develop the platform in an understood regime, but energy remains to explore more parameters.

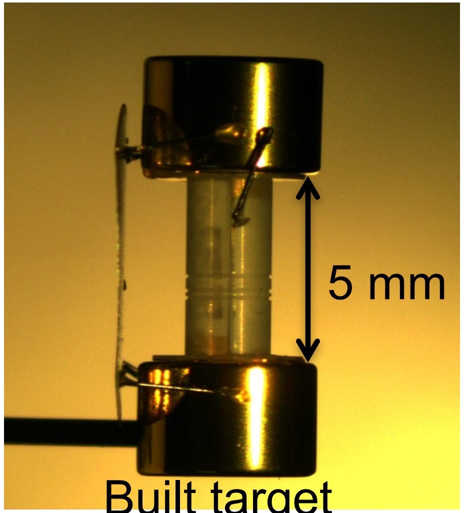

Built target

To scale target designs

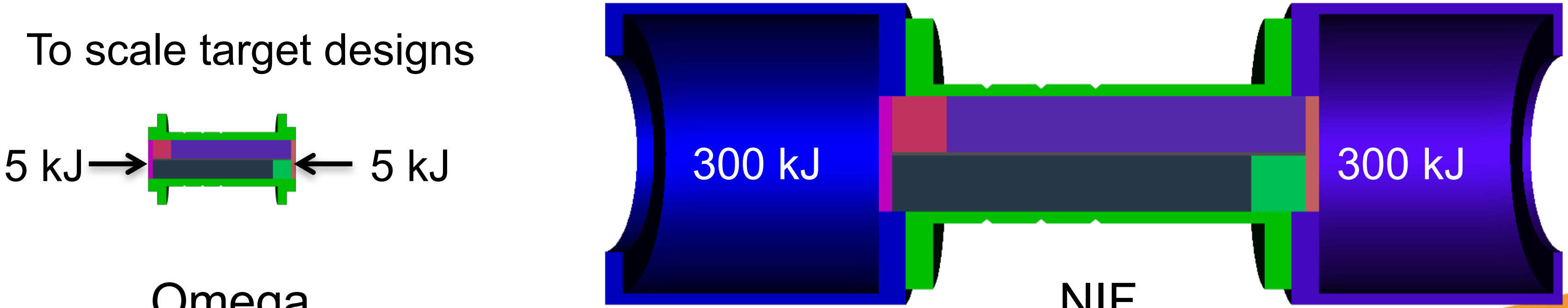

Omega NIF

The NIF-scaled experiment pushes this platform to longer times, with more steady drive

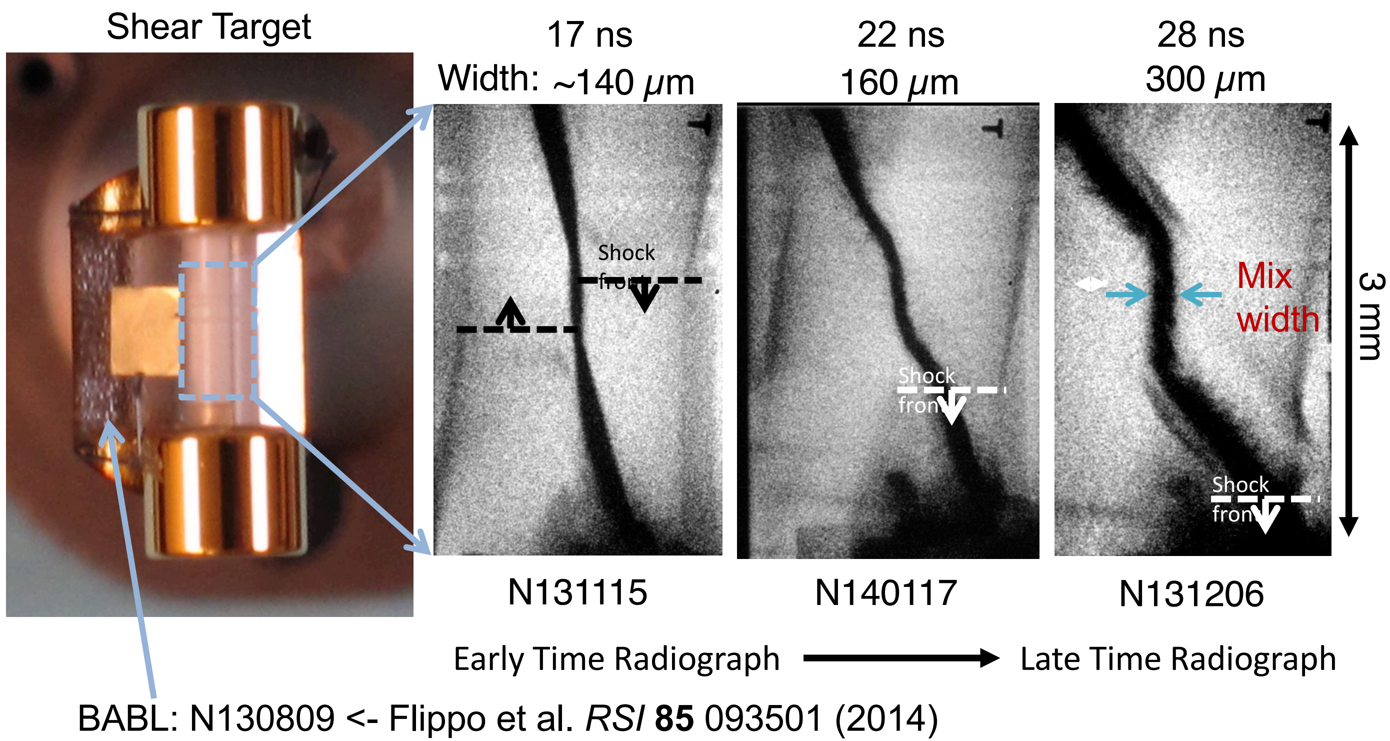

Phys. Plasmas **22**, 056303 (2015)

This provides our baseline target sequence that we are now perturbing away from

Data published in Doss *Phys. Plasmas* **22** 056303 (2015)

16.4 ns, S01-1 **18.6 ns, S01-2** **19.4 ns, S05-1** **20.8 ns,S05-2** **21.8 ns, S03-1**

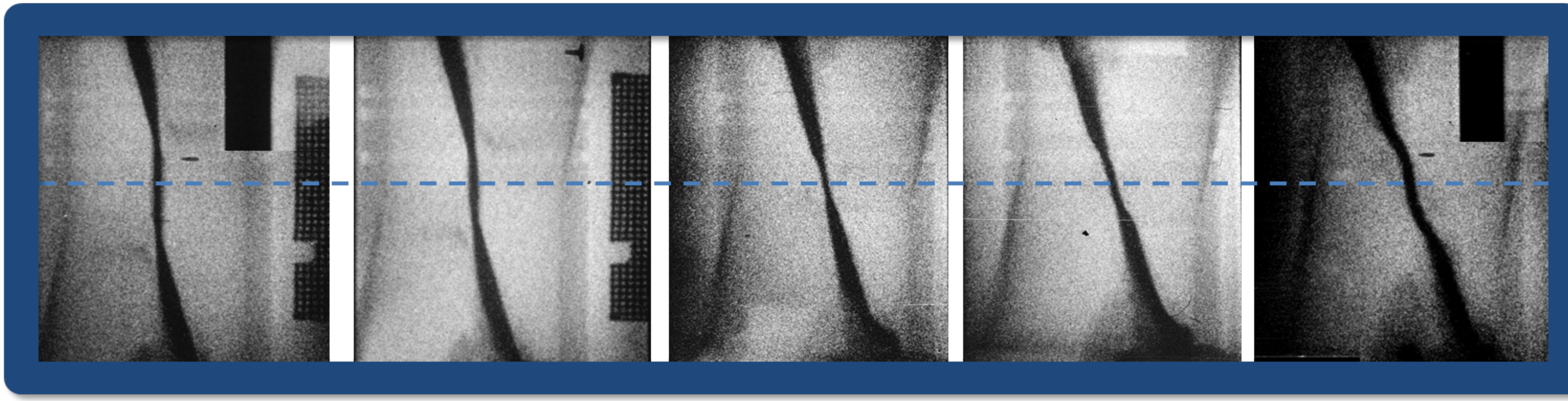

23.0 ns, S03-2 **24.4 ns, S06-1** **25.6 ns, S06-2** **27.2 ns, S02-1** **28.4 ns, S02-2**

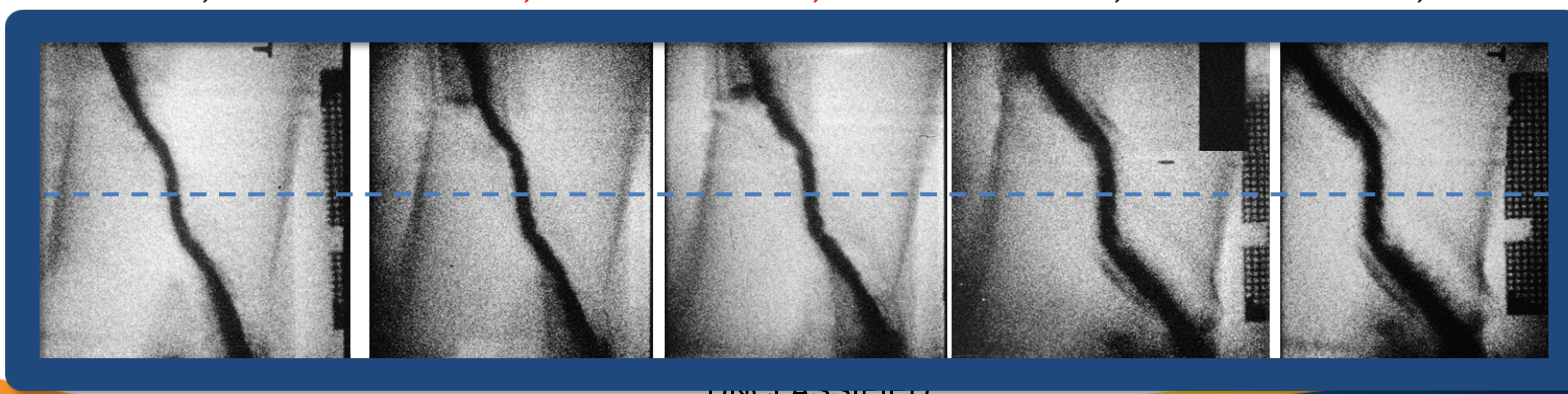

Classical flow morphology is stabilized at the NIF scale

- While the OMEGA experiments demonstrated chaotic patterns (probably due to destabilizing transients and edge effects driving mix by effects in addition to shear), NIF experiments show coherent patterns of isolated shear.

Titanium experiments at each facility

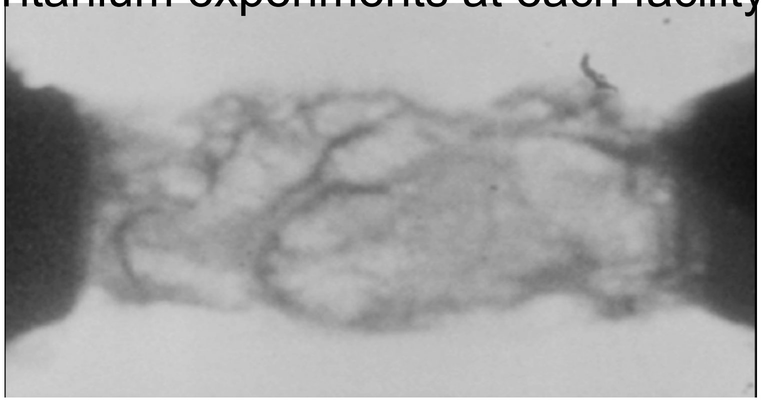

Ω

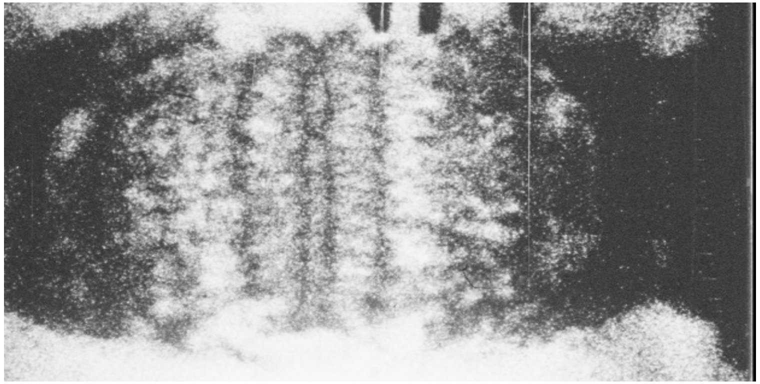

NIF

UNCLASSIFIED

Primary shear instability structures are seen persisting to late times at NIF

- Kelvin-Helmholtz rollers are hinted at in the edge view and are plainly visible in the plan (through the layer) view images.
- Features now look like the classical flows (below)

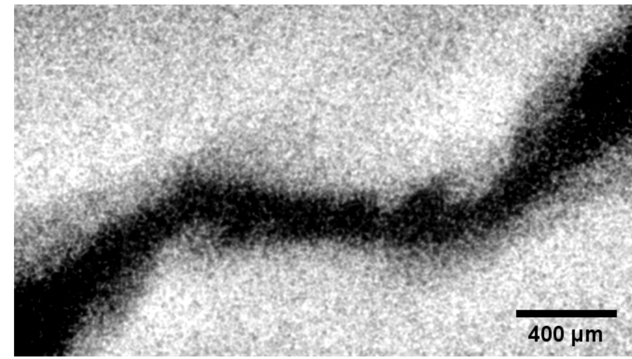

N141006

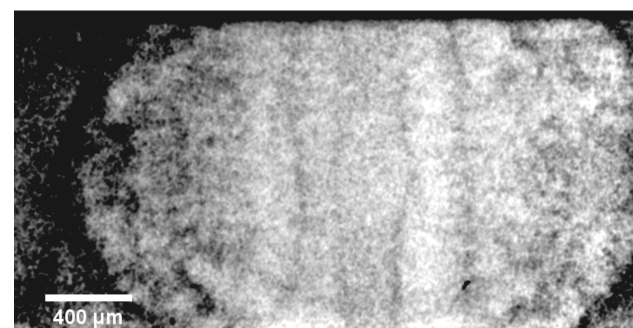

N150527

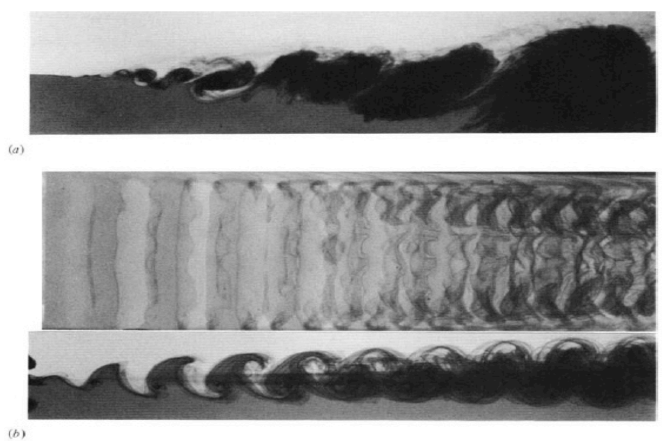

Secondary (3D) shear instabilities are now measurable

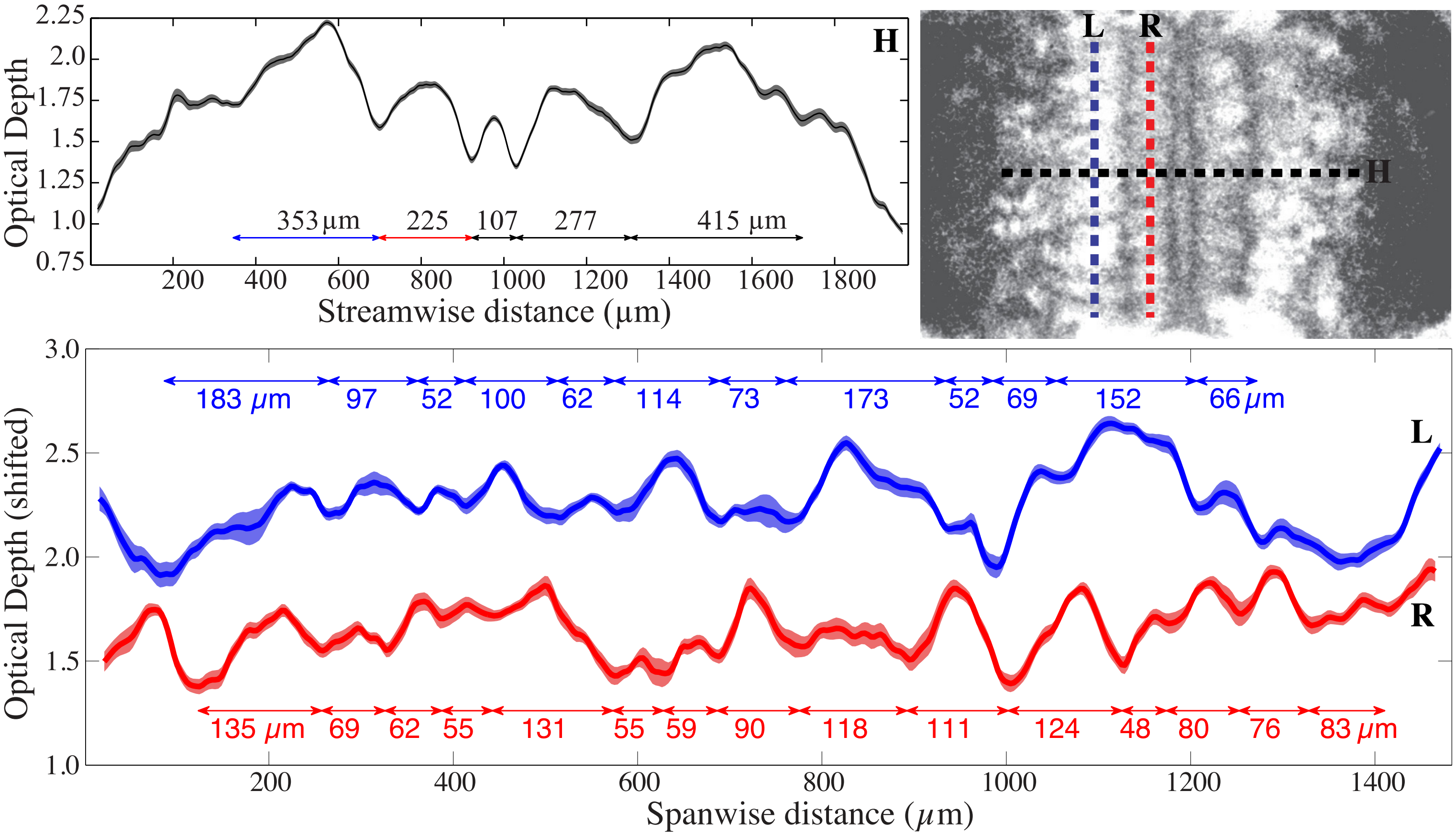

- Lineouts from titanium plan view (N150604) show structure both within and between the KH rollers.
- In ongoing research, higher-order structure in lineouts may inform additional variables.

Phys. Rev. E, **94**, 023101 (2016)

This instability length scale is controlled by small-scale dynamics

R. T. Pierrehumbert and S. E. Widnall, *J. Fluid. Mech* **114**, 59 (1982)
R. T. Pierrehumbert, Phys. Rev. Lett. **57**, 2157 (1986)
B. J. Bayly, *Phys. Rev. Lett.* **57**, 2160 (1986)
M. J. Landman and P. G. Saffman, *Phys. Fluids* **30**, 2339 (1987)
F. Waleffe, *Phys. Fluids A* **2**, 76 (1990)
C. Eloy and S. Le Dizès, *J. Fluid. Mech* **378**, 145 (1999)
P. Meunier and T. Leweke, *Phys. Fluids* **13**, 2747 (2001)

Phys. Fluids, Vol. 13, No. 10, October 2001

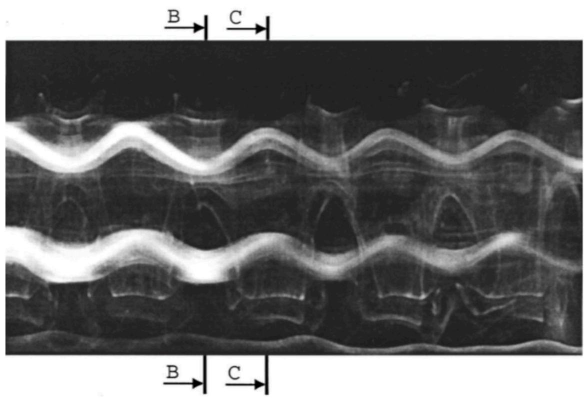

Experimental measurement of vortex filament instability, with a preferred wavelength of ~3.1 times the core size in agreement with the new theory of the elliptical instability

- Originally investigated as a Widnall instability of vortex filaments, subsequent work identified the active mechanism as straining of the irrotational core of the vortex.
- The size of the core is controlled by viscous diffusion* and collisional plasma diffusion would take of order 100 μs.
  - Assume instead a turbulent eddy viscosity to evolve at the appropriate timescale (10 ns) to infer turbulent kinetic energies of order 10^{12} cm^2/s^2, and Re ~ 10^8
  - … or the Braginskii plasma viscosity estimate is off by 80,000 (have ~0.5 mm^2/s, need 40 μm^2/ns)

*(E. Meiburg and P. K. Newton, *JFM* **227**, 211 (1991))

The implied energy is high for a mixing layer, but reasonable for HED

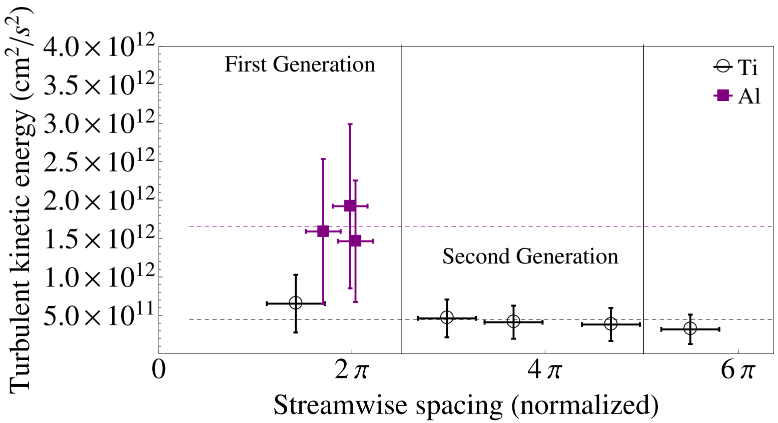

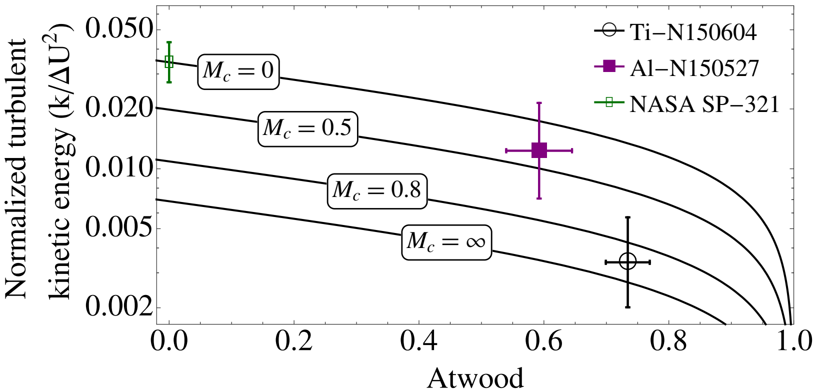

- Analysis of eight lineouts show consistent energy measurements in each shot.
- Inferred energies are broadly consistent with nondimensional scaling for supersonic, high-Atwood mixing layers.
- Titanium inferred to have lower energy conversion to mix than lower-density aluminum.

Phys. Rev. E, **94**, 023101 (2016)

Modeling can match the growth rate of the layers

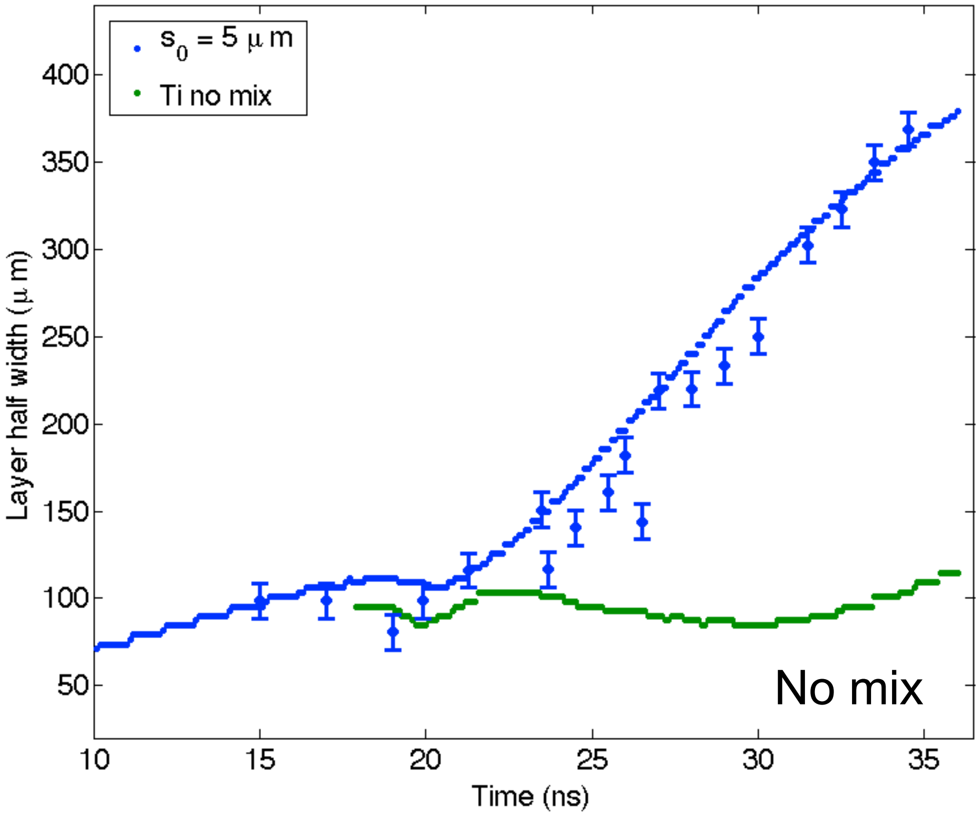

- Shown here is the titanium layer width vs. Simulations with and without the BHR mix model applied.
- A match to layer roughness can be found; the no-mix simulation shows no appreciable growth.

Preliminary measurements

Enhanced roughness targets are now used to control the 3D spectrum at OMEGA and NIF

Targets with intentionally amplified (still 3D broadband) roughness characteristics have been fired at both facilities.

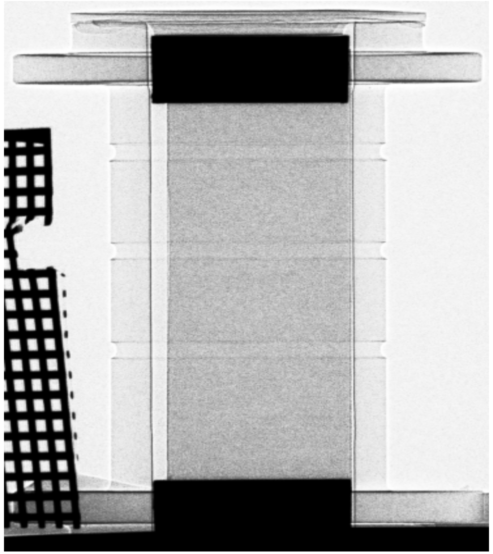

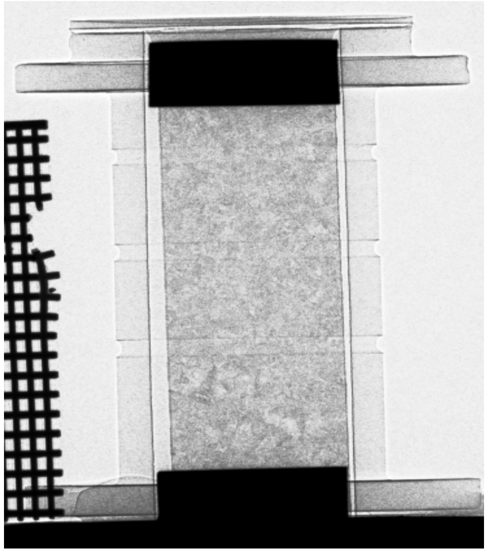

WYCO

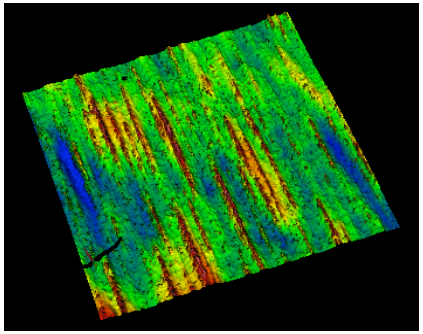

Our typical 40 μm thick aluminum rolled foils have 0.2 μm RMS surface structure.

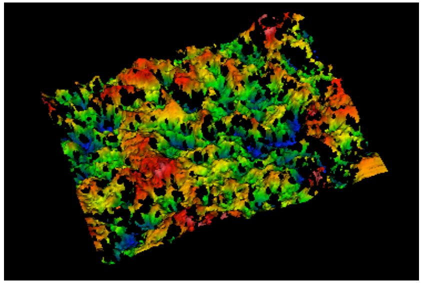

Our roughened aluminum has approx. 5 μm surface RMS with same layer mass.

OMEGA roughened foil analysis and preshot radiographs from Merritt *Phys. Plasmas* **22** 062306 (2015)

Enhancing the roughness at NIF has increased the mixing structure visible to the edge-on view considerably

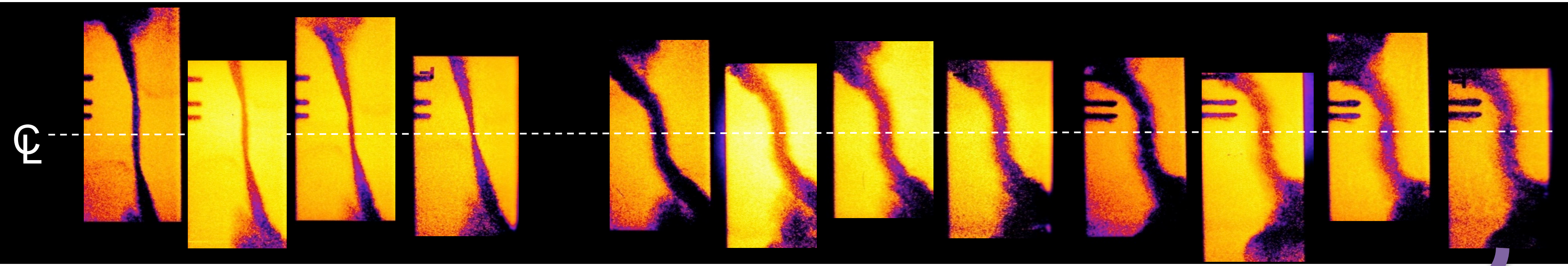

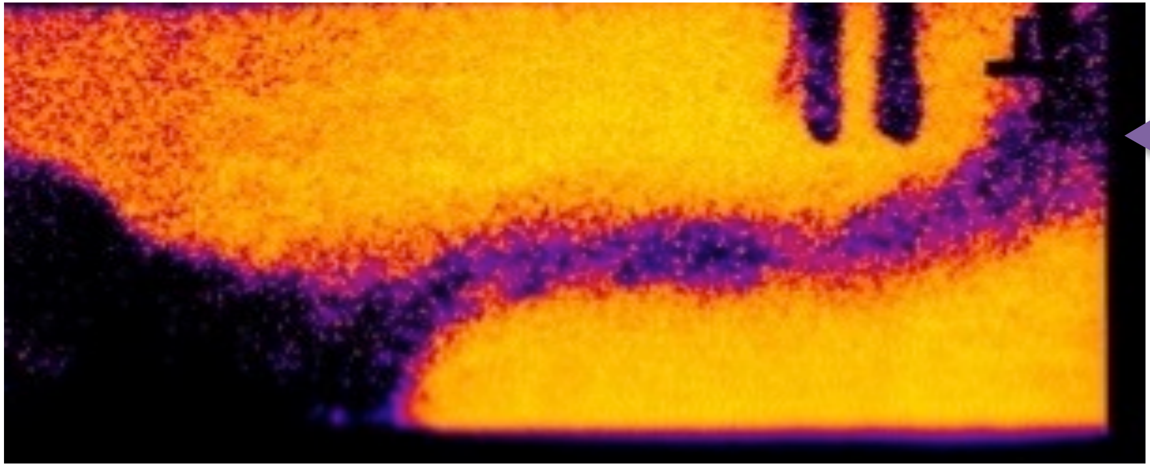

Shots from May/June 2015

- More variation is now visible on top of the roller structures.

Flippo, et al. PRL 117, 225001 (2016)

We have varied density by shooting Titanium, Copper, Vanadium, and roughnesses

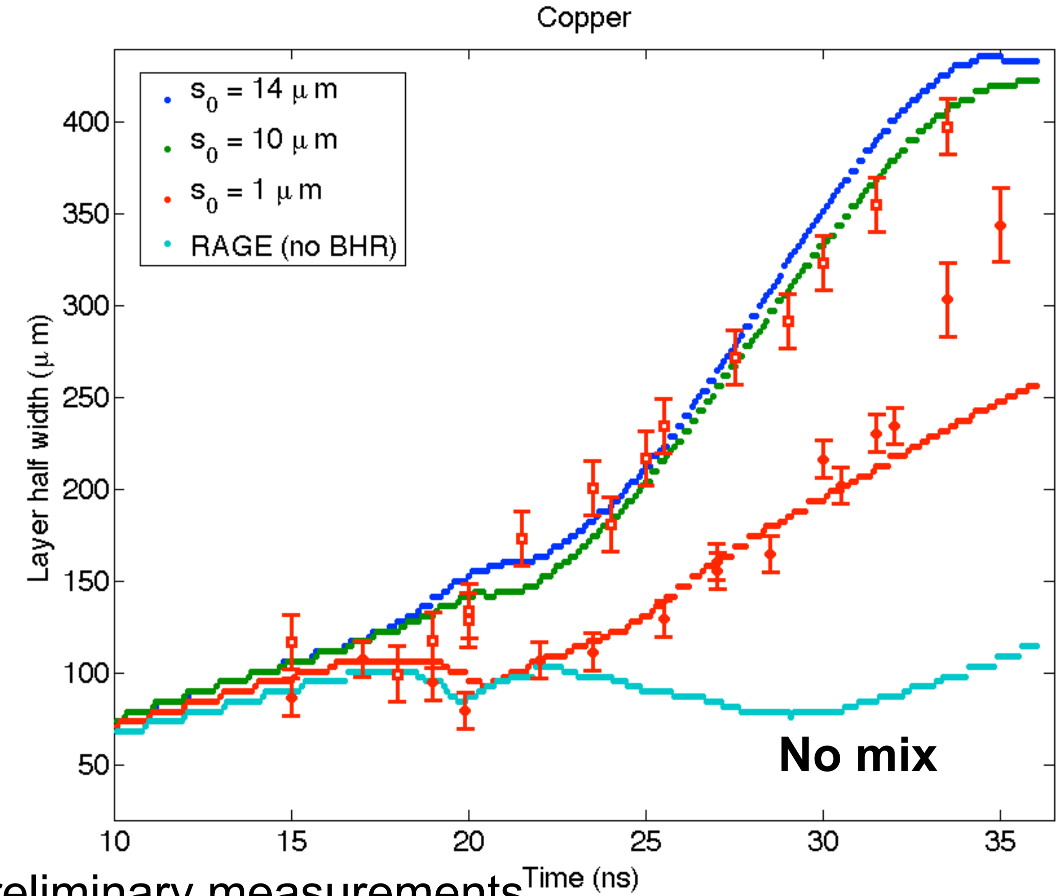

Preliminary measurements

- Shown here is a comparison of four simulations with roughened and smooth Copper vs. data.
- The **only** change between simulations is the change in the BHR roughness parameter.
- A comparison of Al is in [Flippo, Doss, et al. PRL 117, 225001 (2016)]

Complementing the roughness shots, we have also fired imposed perturbation sequences at OMEGA

- Single sine waves impressed into the foil.
  - 100 µm shown
- Lets us map out the linear mode of the instability to complement the nonlinear data.

4 ns
77597

6 ns
77605

8 ns
77601

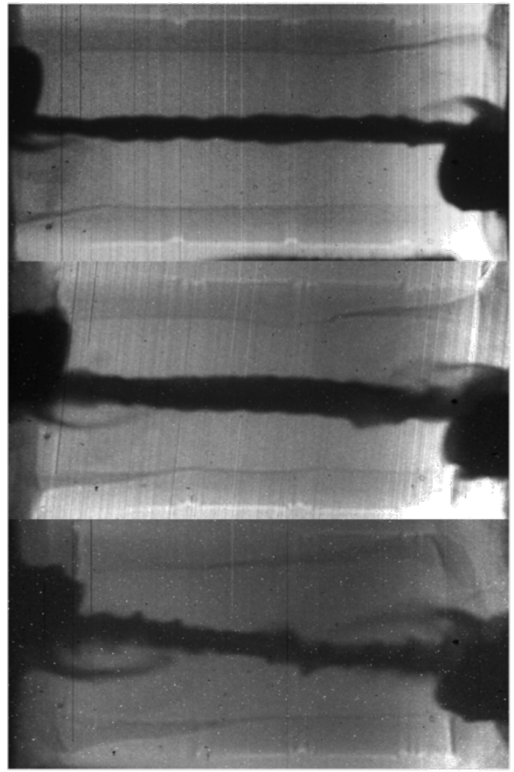

10 ns
77596

12 ns
77604

14 ns
77608

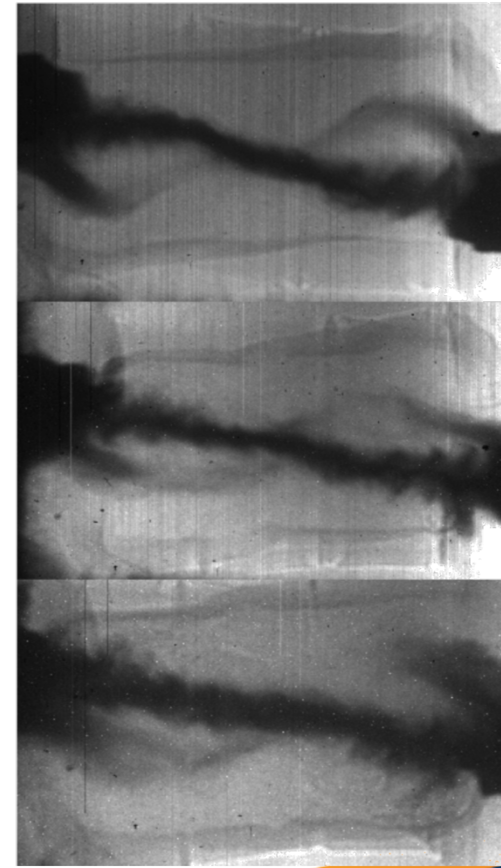

Outstanding questions and future work

- **Complementary to linear-phase instability measurements, these experiments seek to probe the deeply-nonlinearly-saturated limits and their transport properties in the high-energy-density regime.**
  - Relies on primary turbulence theory as developed in the 1970s for low-energy-fluids for comparison. Do plasma effects matter?
  - Radiography of large scale sizes indicates presence of small-scale mixing but does not image them directly. Can x-ray microscopy address?
- **Shear-driven planar mixing layer experiments demonstrate analogous behavior to traditional fluids at observable scales.**
- **How are initial conditions to be treated in HED?** We can locate matches in model initial-length-scale parameters against the roughness of layers, but does a consistent scaling exist?